HYBRID COMPUTATIONAL PHANTOMS OF THE 1, 5, AND 10 YEAR OLD MALE AND FEMALE REFERENCE INDIVIDUALS

By

DANIEL LEE LODWICK

A THESIS PRESENTED TO THE GRADUATE SCHOOL
OF THE UNIVERSITY OF FLORIDA IN PARTIAL FULFILLMENT
OF THE REQUIREMENTS FOR THE DEGREE OF
MASTER OF SCIENCE

UNIVERSITY OF FLORIDA

2008

To my Lord and Savior, Jesus Christ, through whom I am able to accomplish great things.

ACKNOWLEDGMENTS

I thank my research advisor, Dr. Wesley E. Bolch, for his guidance through these last few years and his positive encouragement. I also thank Dr. Choonsik Lee for all of his hard work in helping me to complete this set of phantoms and for introducing me to much of the software that was required to complete this work. I would also like to acknowledge Dr. Choonik Lee for his segmentation of the 5 year voxel phantom. Finally, I thank the National Cancer Institute for supporting this research under grant RO1 CA116743 (subcontract by Rensselaer Polytechnic Institute).

TABLE OF CONTENTS

LIST OF TABLES

LIST OF FIGURES

LIST OF ABBREVIATIONS

CAP	Chest/abdomen/pelvis
CT	Computed tomography
GI	Gastrointestinal
HU	Hounsfield Unit
ICRP	International Commission on Radiation Protection
ICRU	International Commission on Radiation Units and Measurements
IRB	Institutional research board
MR	Magnetic resonance
NCAT	NURBS-based cardiac torso
NURBS	Non-uniform rational basis spline
UFH	University of Florida hybrid

Abstract of Thesis Presented to the Graduate School
of the University of Florida in Partial Fulfillment of the
Requirements for the Degree of Master of Science

HYBRID COMPUTATIONAL PHANTOMS OF THE 1, 5, AND 10 YEAR OLD MALE AND FEMALE REFERENCE INDIVIDUALS

By

Daniel Lee Lodwick

May 2008

Chair: Wesley E. Bolch
Major: Nuclear Engineering Sciences

Traditionally, computation of radiation dose to individuals was calculated using a host of stylized phantoms. These phantoms were easily used and manipulated, but lacked anatomical realism of organ shape and position. More recently, tomographic phantom construction was made possible through advances in computer technology. The explicit segmentation of CT or MRI images led to this phantom series that maintained anatomical realism, but lacked the versatility of stylized phantoms. A new class of phantom has been introduced that maintains anatomical realism and allows for non-uniform deformation of organs. This "hybrid" phantom utilizes both NURBS and polygon mesh surfaces to describe the complex geometries of internal organ shapes.

This new technology was used in the effort to create hybrid phantoms of the 1, 5, and 10 year male and female phantoms. After selection of the CT data, the hybrid phantoms were created through the four steps, which are (1) image segmentation, (2) polygon mesh modeling, (3) NURBS modeling, and (4) standardization. Standardizing of each phantom was performed by matching anthropometric data, alimentary tract length data, and ICRP 89 reference organ mass data. The targeted tolerance for anthropometric and alimentary data was 5%, whereas the targeted tolerance for matching of organ mass was only 1%. With the exception of the thymus

for the 1 year old phantom, all organs were matched in the hybrid phantoms within 1%. All anthropometric data were matched within 5% as well as the alimentary tract lengths (except for the left and right colon of 1 year old phantom). It is important to note that in the voxelized phantom, skin mass was not matched within 1% for any of the phantoms.

Development of the 1, 5, and 10 year UFH phantoms has shown the range of scalability, as well as the potential for use in phantom modeling. These models serve as the standard for radiation dose assessment for reference individuals, and they will also be the starting point for expanding research into the difference in radiation dose to non-reference individuals.

CHAPTER 1
HISTORY OF PHANTOM DEVELOPMENT

Introduction

Analysis of radiation risk in the human body requires knowledge of the absorbed dose to organs. However, radiation dose is not directly measurable in the body. For this reason, phantoms are used to estimate the doses in real individuals. Two methods exist including taking direct measurements in physical phantoms and using Monte Carlo radiation transport to calculate the absorbed dose to organs in an anthropomorphic computational phantom. A computational phantom is a 3D model of the all internal organs and the outer body contour. The goals of a good computational phantom are: anatomical realism, versatility, and having internal organ masses consistent with standards set by the International Commission on Radiation Protection (ICRP)

The two main types of computational phantoms that are traditionally utilized are stylized (mathematical) phantoms and voxel (tomographic) phantoms. While both have distinct and positive aspects that highlight their usefulness in radiation dose calculation, each presents specific problems that are drawbacks to their use. Therefore, neither of these two types of phantoms are able to satisfy all of the desired characteristics of a computational phantom. The hybrid phantom was developed in order to combine the best characteristics of each of these phantoms.

Stylized Phantoms

Stylized phantoms use mathematical shapes and surfaces (spheres, ellipses, toroids, etc.) to estimate all internal organs and the outer body contour. These phantoms provide an easy to use phantom that is non-uniformly deformable through simple parameter modifications. This type of phantom was first created by Oak Ridge National Laboratory as an adult male model (Snyder *et al*. 1969). This phantom was later expanded to include the male and female adult

phantoms (Kramer *et al*. 1982) and a series of pediatric phantoms (Cristy and Eckerman 1987). Stylized phantoms were also generated to represent pregnant females at the end of each trimester of gestation (Stabin *et al*. 1995).

These phantoms have the flexibility of changing individual organ masses, which allows the phantoms to correlate to reference values. However, despite all of these organs having the correct anatomical mass, the organs lack the correct anatomical shape and position. Furthermore, organ pairs in close proximity (e.g., liver and stomach) should be nestled against each other, but the shapes of the stylized organs do not permit for the organs to be placed in such close proximity. The more complex contours that are required to realistically model organ shape were too advanced for the computer technology when these phantoms were created in the 1980's.

Voxel Phantoms

As computer technology advanced, a new format of voxel phantoms was created. Voxel phantoms use image sets from CT or MRI imaging of live or deceased patients and thereby maintain realistic organ depth and position. The organs are visually identified and segmented on the image sets. The result is a large array of voxels, each with a specific tissue and material label. However, there are several drawbacks to this methodology that must be considered.

One issue is that each voxel phantom is modeled directly after an image set of a patient. Therefore, once the model is complete, the phantom is patient-specific to the particular patient from whom the image data were obtained. The only method for scaling of these phantoms is to uniformly scale the entire phantom by changing the voxel dimensions for every voxel in the matrix. There is no process by which to scale individual organs in order to match reference organ masses. This process was previously used by several groups (Kramer *et al*. 2004a, b; Nipper *et al*. 2002; Pazik *et al*. 2007). Additionally, voxel phantoms require significant time to create.

Each phantom is manually segmented from a set of axial slice images and each pixel of each slice is tagged as a particular organ or tissue, which is a very labor intensive process.

Another issue with the creation of voxel phantoms is that there are several organs in CT images that are not always identifiable. This problem is usually found in soft tissue organs that cannot be identified due to contrast resolution issues. For example, delineating the exact boundaries of the pancreas in relation to the stomach and intestines can prove too challenging even for an experienced radiologist. This problem is further exacerbated in pediatric image sets where operating characteristics are usually tailored to decrease dose at the expense of image resolution. Furthermore, MR imaging, which would provide better soft tissue resolution, requires longer time for image acquisition and has higher risk of patient motion and image blur. Pediatric patients may not even be considered for imaging procedures using this modality as it would often require anesthesia, which adds significant risk to the patient.

Hybrid Phantoms

A new type of phantom that is coming into wide popularity is the hybrid phantom. The term hybrid was developed to describe the nature of the phantom as having the benefits of both the stylized and voxel phantoms. These models utilize the advances in computer graphics and modeling for the purposes of accurately describing human anatomy while maintaining flexibility of use. The hybrid models contain non-uniform rational basis spline (NURBS) surfaces to describe most organs and polygon mesh surfaces to describe other organs.

The NURBS technology was previously developed for modeling of a 4D phantom for image correction of cardiac motion in nuclear medicine imaging (Segars *et al*. 1999). The versatility of use of these surfaces was highlighted in this NURBS-based cardiac torso (NCAT) phantom. The spline surfaces were created to model the internal organs of the torso and were manipulated easily through movement of control points to simulate the contraction and

relaxation of the heart at several time steps (Segars *et al*. 2002). Subsequently, this technology was employed to transform the UF voxel newborn female phantom (Nipper *et al*. 2002) into the UF hybrid newborn male and female phantoms (Lee *et al*. 2007).

The NURBS technology allows for individual organ mass matching through non-uniform deformation. Because these phantoms also utilize CT or MR images of patients, they maintain anatomical realism of organ shape and position. Thus the reference "hybrid" phantom is one that utilizes the realistic image data while maintaining the versatility of the free deformation and matching the reference mass for each organ as defined by the ICRP.

CHAPTER 2
DESCRIPTION AND DEVELOPMENT OF HYBRID PHANTOMS

Computed Tomography Data Collection

The development of hybrid phantoms can be separated into four distinct steps: image segmentation, polygon mesh modeling, NURBS modeling, and voxelization. Before beginning image segmentation, sets of CT image data must be selected. The CT image data archive at the Department of Radiology at Shands Children's Hospital at the University of Florida was searched by Dr. Choonsik Lee under the approval of the Institutional Research Board (IRB) and through HIPAA-compliant practices. Several scans of pediatric patients were selected based upon the age of the patient at the time of examination, the anatomical regions of coverage and the axial slice resolution of the scans. After selection of these scans, each examination was reviewed by a pediatric cardiologist, Dr. Jonathan Williams, to ensure that each patient exhibited normal anatomy and did not contain any disease or surgery that would otherwise alter the size or position of the internal organs.

Finalized data were a collection of 6 CT examination studies: 3 chest/abdomen/pelvis (CAP) and 3 head examinations. Two of the head examinations also contained ultra high resolution images of the cervical spine at 0.75 mm slice thickness. The data were chosen to yield a CAP scan and a head scan as near as possible to each of the target ages (1, 5, and 10 years). Each head and torso pair were segmented separately and were not combined until the later stages of phantom development. Also, high resolution images were obtained of an 18 year old male cadaver at 1.0 mm slick thickness. The scans used were of the left arm and left leg, which contained 1098 slices and 819 slices, respectively. The imaging and patient parameters of the CT image sets are summarized in Table 2-1.

Image Segmentation

The segmentation was performed using *3D-DOCTOR*™ (Able Software Corp., Lexington, MA, USA). The skeletal tissue of head and torso regions were segmented semiautomatically using brightness thresholding. First, the *Interactive Segmentation* feature was employed and a Hounsfield Unit (HU) threshold was determined by visual inspection of image slices. Next, all slices were automatically segmented using the HU threshold previously determined and all pixels with a HU value larger than that threshold were included. This automatic segmentation was manually reviewed to ensure correctness. The most common problem that had to be manually corrected was in the spongiosa region of the bone. Many times in the phantom, certain regions of the spongiosa that contain higher concentration of bone marrow and lower concentration of ossified trabecular bone are below the HU threshold and must be manually added to the segmented bone tissue. This problem is particularly evident in the vertebrae, where there is a very thin layer of cortical bone. Several of the vertebrae were segmented entirely by manual segmentation.

After bone segmentation, regions are segmented in the spaces between the vertebral bodies to represent intervertebral disks. However, the axial resolution of each head scan was too large to allow for explicit segmentation of the cervical intervertebral disks. Therefore, high resolution image sets of the cervical spine were segmented from the 2.3 year old and 12.3 year old datasets (Fig. 2-1). The 2.3 year old c-spine was scaled to fit the 1 year and 5 year phantoms, while the 12.3 year old c-spine was scaled to fit the 10 year phantom. At this juncture, the skeleton of each phantom contained a complete head and torso, but no arms and legs. An additional dataset was used of an 18 year old male cadaver. The bones of the left arm and leg were segmented at 1.0 mm slice thickness to be attached to the phantom at a later stage.

As for construction of the 5 year old phantom, the UF voxel phantom of a 4 year old male patient was utilized (Lee *et al*. 2006). The voxel model was imported into the *3D-DOCTOR* software and segmented in the same manner as the 1 and 10 year phantoms. The only change to the original segmentation was the inclusion of intervertebral disks.

Unlike bone tissue segmentation, the internal organs are almost exclusively segmented by manual segmentation. One exception to this is the lungs. For the lungs, a threshold technique is again used, except that the region included has a HU value less than the threshold value. All other organs are segmented manually using the nodal segmentation method of *3D-DOCTOR*.

Traditionally image segmentation is performed by tagging each pixel of each image as belonging to a particular organ. However, the nodal segmentation method utilizes nodes that are placed in sequence on the outer boundary of the organ and each node is connected to the next by a line. This line is ultimately closed once the entire boundary of the organ has been defined, which yields a contour of the organ in that image plane.

Polygon Modeling

After every organ has been segmented in *3D-DOCTOR*, there is a set of contours for each organ defining the outer boundaries in each image. The *3D Rendering* function is used to render three dimensional structure that fits the contours of each organ. The structure that is created is a polygon mesh. There are two options for this rendering, *Complex Surface* and *Simplified Surface*. The *Simplified Surface* is dramatically smoothed, which does not faithfully represent the original segmentation and alters the resulting organ shapes. The *Complex Surface* option was used because it is a genuine rendering of the segmentation. After rendering, the polygon mesh model was exported into a Wavefront Object file format. This file format contains information on location of each polygon and the corresponding organ tag. The polygon mesh model was

subsequently imported into *Rhinoceros*™ (McNeel, Seattle, WA, USA) for construction of NURBS surfaces.

Non-Uniform Rational Basis Spline Modeling

Much of the internal organs in polygon mesh format are directly converted to a NURBS surface. This was achieved by lofting a surface over the contours of the polygon mesh. However, not all organs could be represented by NURBS surfaces. For example, the brain was not converted to a NURBS surface because the brain is encased in the cranium. If a smoothed surface were generated for the brain, then there would be overlapping regions between the brain and the cranium due to the roughness of the cranium.

Several organs were not clearly identifiable on the CT images. Therefore, stylized shapes were generated to model these organs. The position of each organ was determined using anatomical landmarks. For example, the thymus was positioned superior to the heart and was bounded by the lungs, clavicles, trachea and thyroid.

Skeletal Modeling

The skeleton is another organ that cannot be represented by NURBS surfaces. The spline surfaces are not able to model highly complex structures as it would require too many input parameters to create a smooth spline surface. For example, the vertebrae are exceedingly complex in shape and, as such, are left in polygon mesh format. In fact, the only bone site that is modeled by NURBS surfaces is the ribcage.

In order to model the ribcage, the center track of each rib was specified with a curve and several cross sections were taken along the length of the rib in order to create a pipe along the central track with the same cross section. It was necessary to use more than one cross section through the rib as the rotation of the curve from the vertebrae to the costal cartilage caused a rotation of the cross section about the central track. This resulted in several segmented surfaces

representing each rib. The segments were blended using the function *Merge Surface* and the resulting tube-like surface was closed on the ends using the *Cap Planar Holes* function.

Additionally, the costal cartilage was generated using the skeletal structure and a priori anatomical knowledge because it is not visually distinguishable from the muscle surrounding the ribcage in the CT data. The central track for each rib was extended to reach from the end of each rib towards the sternum and the contour of each rib was used for cross sectional shape to generate the volume of the cartilaginous portion of the ribcage (Fig. 2-2).

Alimentary Tract Modeling

The tortuosity and close proximity of the alimentary tract, coupled with the low contrast between much of the soft tissue in the abdomen, make direct conversion of segmented organs into NURBS surfaces a poor method of modeling. For the stomach, the NURBS surface was created and the control points were manipulated such that the shape and position of the organ were matched. Because of the variability in stomach shape and position from person to person, in addition to the variation due to food intake, both the original segmentation and supplemental anatomical literature (Zhang 1999) were utilized in creation of the NURBS stomach surface. As for the esophagus, small intestine, and colon, two pipes (one for the outer wall, one for the inner wall) were fit to the central track of the lumen.

Standardization of Phantoms

A significant benefit to hybrid phantom development is the versatility to match the phantom to a host of reference values. This allows not only for standardization of dosimetry calculations to that of a reference individual, but also allows for modifying the phantom to match individual variations in body morphometry for reconstructive radiation dose calculations.

Anthropometric Data Matching

The next step of development was to match the following reference anthropomorphic values:

- Sitting height
- Standing height
- Cranial circumference
- Arm length
- Buttock circumference
- Biacromial breadth
- Neck circumference
- Waist circumference

It is important to note that the values of biacromial breadth, and buttock, neck, and waist circumference were not available for the 1 year old individual. Therefore, only 5 and 10 year phantoms are matched to these parameters.

The reference values for these measurements were reported by several sources. The standing height was provided by ICRP Publication 89 (ICRP 2002). The sitting height, biacromial breadth and buttock circumference was provided from the third National Health and Nutrition Examination Survey (NHANES III) that was conducted by the Centers for Disease Control (CDC) (http://www.cdc.gov/nchs/nhanes.htm). The fourth NHANES yielded reference values for waist circumference for 5 and 10 year phantoms. The reference values for arm length, head circumference, and neck circumference were obtained from the *Anthrokids* project by the US Consumer Product Safety Commission (CPSC) in the late 1970's (http://www.itl.nist.gov/div894/ovrt/projects/anthrokids).

The reference values for these measurements were reported by several sources. The standing height was provided by ICRP Publication 89 (ICRP 2002). The sitting height, biacromial breadth and buttock circumference was provided from the third National Health and Nutrition Examination Survey (NHANES III) that was conducted by the Centers for Disease Control (CDC) (http://www.cdc.gov/nchs/nhanes.htm). The fourth NHANES yielded reference values for waist circumference for 5 and 10 year phantoms. The reference values for arm length,

head circumference, and neck circumference were obtained from the *Anthrokids* project by the US Consumer Product Safety Commission (CPSC) in the late 1970s (http://www.itl.nist.gov/div894/ovrt/projects/anthrokids).

Furthermore, several anthropometric values for the alimentary tract were matched to reference values given in ICRP Publication 100 (ICRP 2006). These values included reference lengths for esophagus, small intestine, right colon, left colon, and rectosigmoid colon (Table 2-2). It was assumed that right colon was defined as the ascending colon plus the first half of the transverse colon and the left colon was defined as the second half of the transverse colon and the descending colon (up to the rectosigmoid).

Organ Mass Matching

After matching anthropometric reference values, all organs were scaled to match the reference mass as defined by ICRP reference (ICRP 2002) within 1% (Tables 2-4, 2-5, 2-6). In order to determine the mass of each organ in the phantom, reference densities were obtained from the International Commission on Radiation Units and Measurements (ICRU) Publication 42 (ICRU 1992).

A major challenge in organ mass matching was found with the scaling of the skeleton. After matching anthropometric values, the change in skeletal volume was realized through use of the *Smooth* and the *Offset Mesh* functions. However, the cranium could not be modified without intensifying the holes found on the inferior portion of the cranium, as well as the socket of the eye and in the temporal bone. These holes originate in the segmentation due to the large in-plane shift in location relative to the axial resolution. This was corrected through image resegmentation in 3D-DOCTOR. Each slice of the cranium was thoroughly reviewed using the feature *Overlay Neighboring Boundaries* in order to visualize and correct the locations where neighboring

boundaries do not overlap (Fig. 2-3). Results of this resegmentation on the cranium are shown in Fig. 2-4.

However, not all organs were able to be matched with 1% precision. For each phantom, the thymus was created to fill the space that was bounded by the thyroid, trachea, lungs, clavicles, and heart. Therefore, the largest volume that the thymus can occupy is found when its surface is abutting each of the neighboring organs. For the 1 year old phantom, the thymus was abutting the neighboring organs and could not be expanded any further, but was still below reference mass by 46.5%.

Furthermore, after the reference lengths for the alimentary tract (ICRP 2006) were matched, the pipe diameter was adjusted to match the reference mass (ICRP 2002). It is important to note that for the 1 year old phantom, the reference mass for left colon was equal to that of the right colon, but the reference lengths were 18 and 21 cm, respectively. Therefore, it was not possible to divide the large intestine such that the length was matched within 5% and the mass matched within 1%. Therefore, the colon was split such that the mass was correctly matched, and the resulting errors in the length of the left and right colon were -7.8% and 8.4%, respectively (Table 2-2).

Additionally, the reference gastrointestinal (GI) content from ICRP 89 was not matched using the densities from ICRU 46. The volumes of GI content that would be unrealistically large using these values and it proved too difficult to be modeled. Therefore, an effective content density was utilized so that the reference content mass would be matched.

After matching the individual organs of each phantom, the total body mass was matched through manipulations of the outer body contour. The tissue within the outer body contour and outside of all of the organs was termed residual soft tissues (RST). This region includes fat,

muscle, lymphatic tissue, blood vessels, some bone-associated cartilage, and other connective tissues. The density and composition of this region was determined as a volume-weighted average of these component tissues in this region.

Creation of Complimentary Gender

The reference values given for the 1, 5, and 10 year individual specified by the ICRP are not delineated into specific male and female values. The gender specific separation of anatomy was assumed to be insignificant for prepubescent individuals, which is supported by other studies (e.g. Slyper 1998). Therefore, the creation of the gender compliment of each phantom was created through the removal of sex specific organs from the originally segmented phantom and insertion of sex specific organs of the opposite gender. This not only allowed for creation of phantoms for which no CT data was readily available, but also maintained uniformity for each gender-pair of phantoms. By utilizing this, any radiation dose differences calculated may be directly attributable to differences in gender.

Voxelization

The ultimate goal of these phantoms is their input into a Monte Carlo radiation transport code for calculation of radiation dose. However, no Monte Carlo code exists that can perform this calculation using NURBS or polygon mesh surfaces. Therefore, the NURBS and polygon mesh surfaces of the hybrid phantom must be voxelized. The voxelization process effectively converts all of the surfaces of the phantom into an array of voxels, each with a specific organ and tissue tag. The algorithms by which the in-house MATLAB code *Voxelizer* operates is described in a previous study (Lee *et al*. 2007).

The first step of voxelization was to export the hybrid model from *Rhinoceros* using the *Raw Triangles* format at a meshing tolerance of 10 degrees. This was selected according to a study on the effect of volumetric discrepancies due to the density of polygons used to describe

surfaces (Lee *et al*. 2007). The voxel resolution of each phantom was selected such that it was small enough to model the skin because it is the thinnest structure in the phantom. The resulting isometric voxel resolution was 0.663 x 0.663 x 0.663 mm^3, 0.697 x 0.697 x 0.697 mm^3, and 0.824 x 0.824 x 0.824 mm^3 for the 1, 5, and 10 year phantoms, respectively. After voxelization, the outermost voxels of the phantom were reassigned to skin tissue. The resulting voxelized organ masses were calculated through counting of the voxel volumes and compared to the reference values from ICRP (Tables 2-4, 2-5, 2-6).

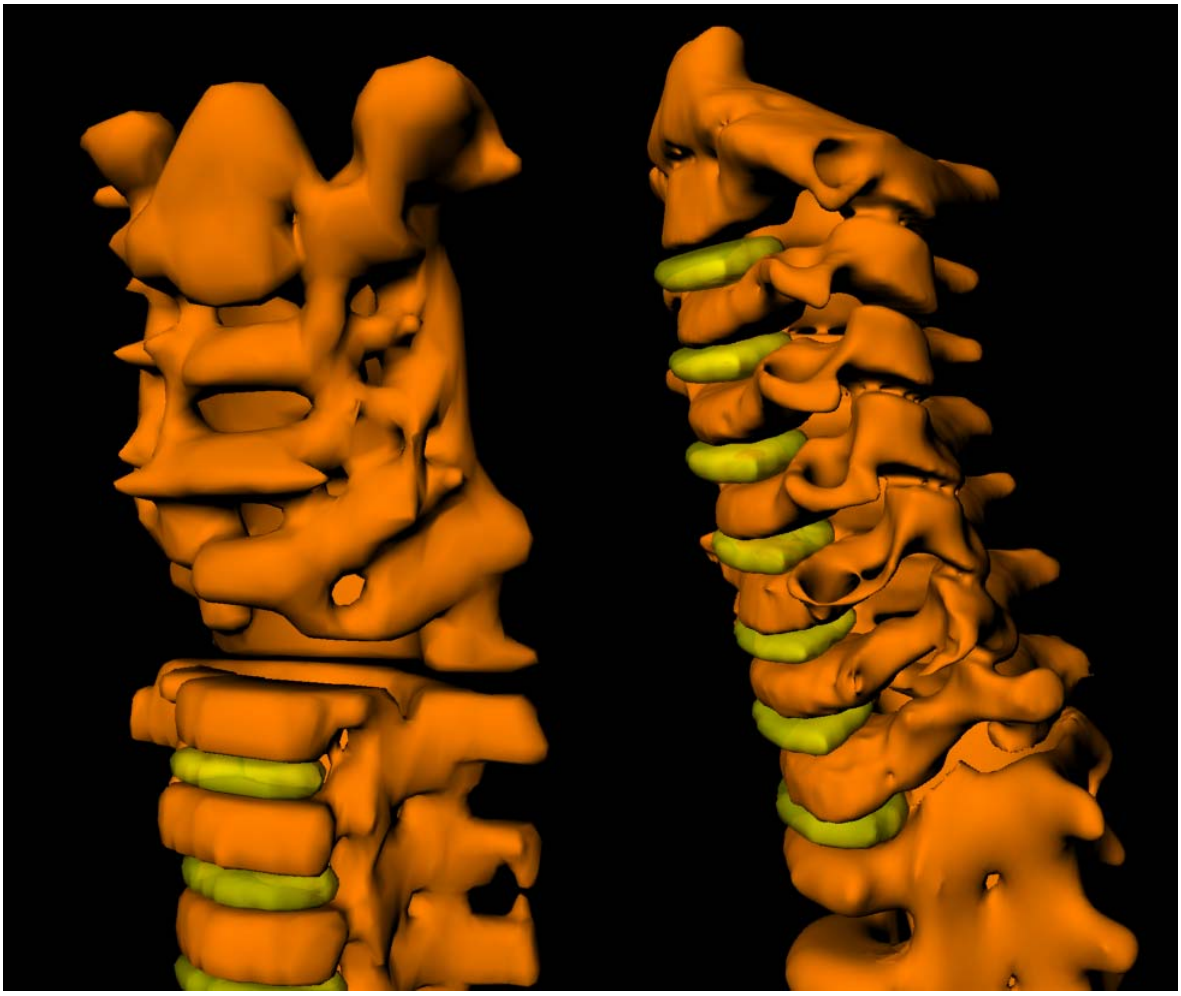

Figure 2-1. Left anterior oblique view of originally segmented cervical spine (left) and high resolution cervical spine (right) for 1 year old phantom. Ossified tissue is represented in orange and nonossified tissue (cartilage) is represented in yellow.

Figure 2-2. Example of costal cartilage modeling in hybrid phantoms. This shows the ribcage for the 1 year old phantom. Ossified tissue is represented in orange and nonossified tissue (cartilage) is represented in yellow.

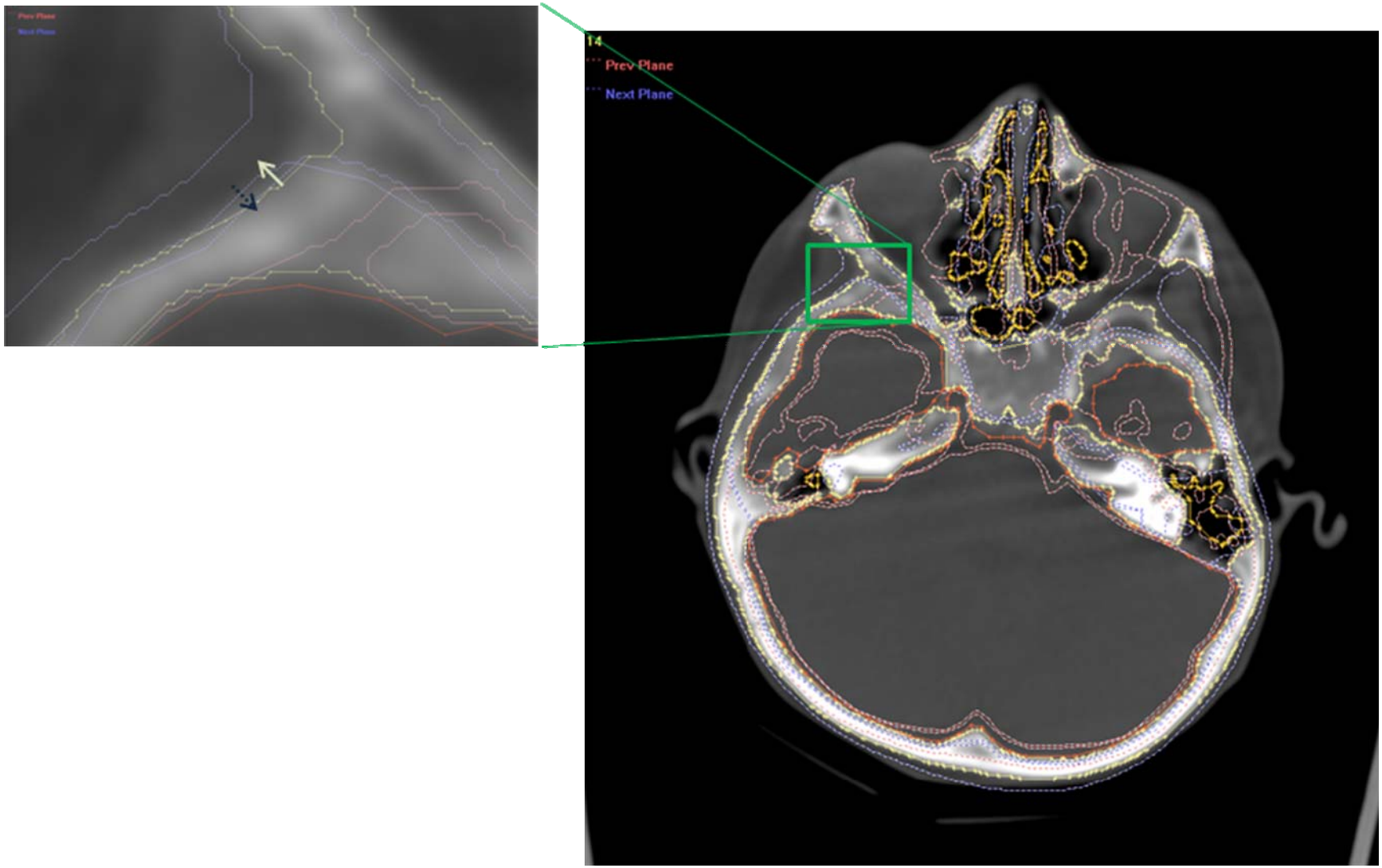

Figure 2-3. Resegmentation of cranium using 3D-DOCTOR. This individual node points are moved in order to maintain overlap between the current slice boundaries and the neighboring slice boundaries. The white arrow in the left window indicates the movement of the current slice boundary and the dotted blue arrow indicates the movement of the next slice boundary.

Figure 2-4. Originally segmented (top) and resegmented (bottom) models of the 1 year old cranium.

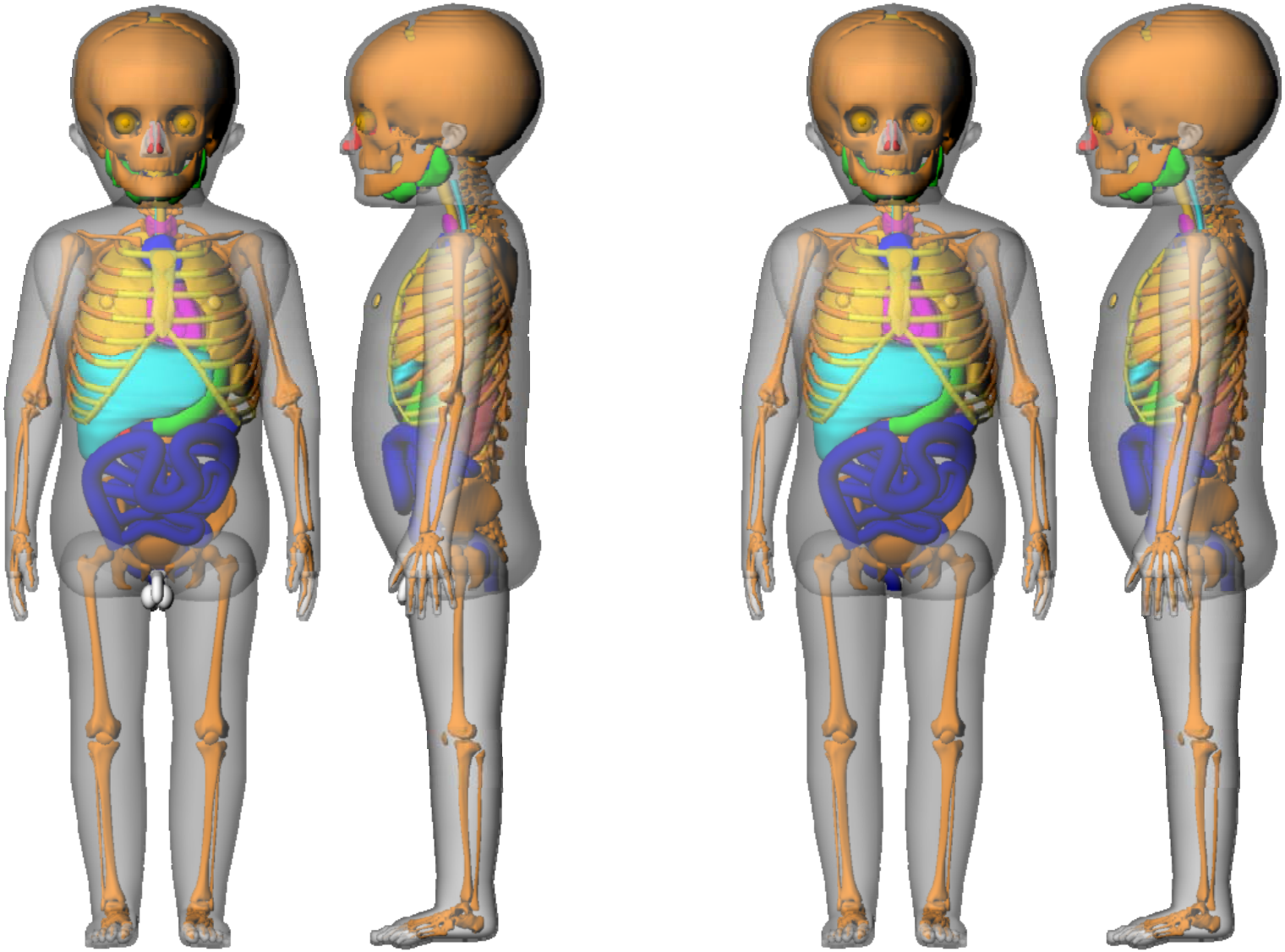

Figure 2-5. Anterior and lateral views of the 1 year male (left) and female (right) phantoms.

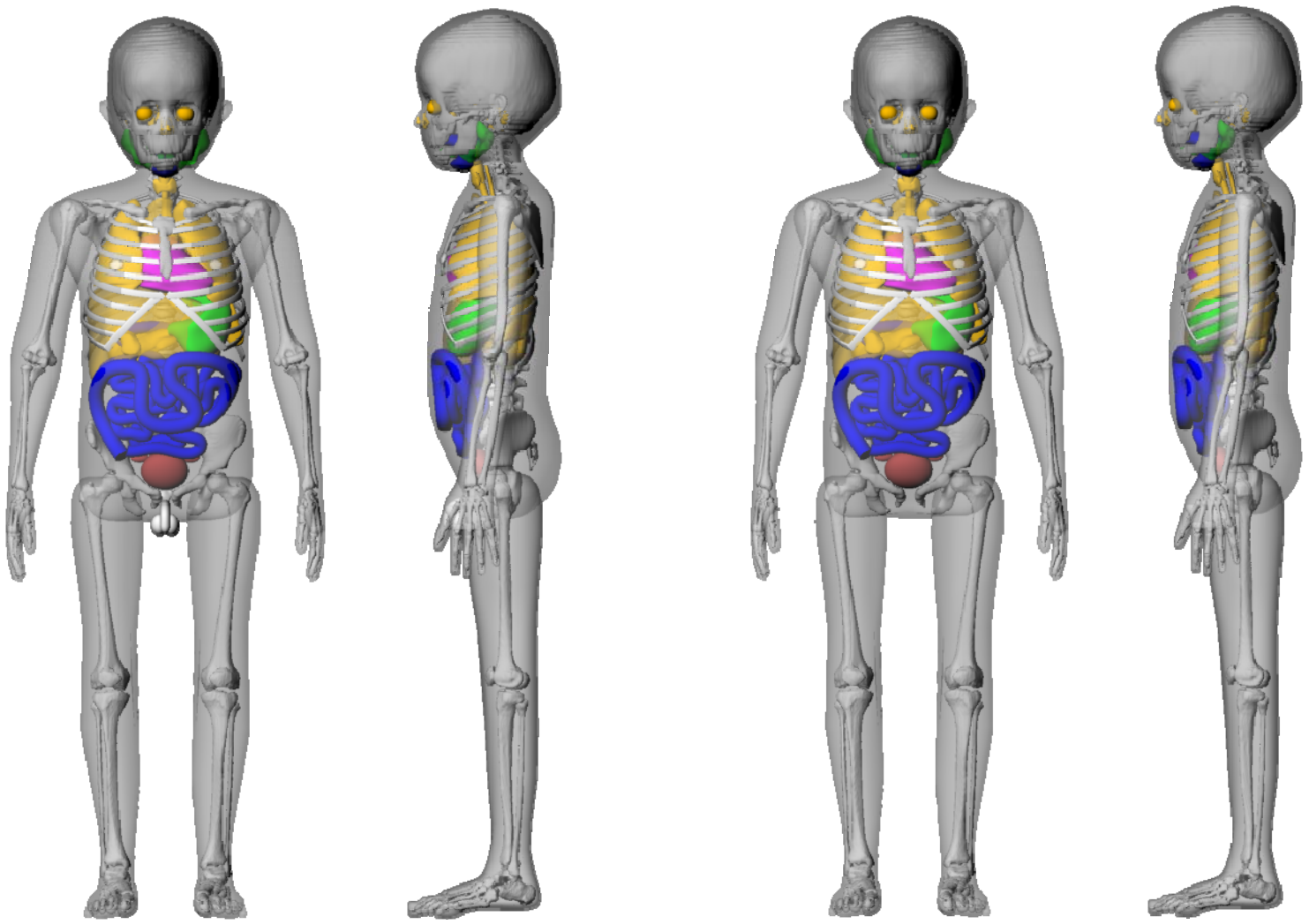

Figure 2-6. Anterior and lateral views of the 5 year male (left) and female (right) phantoms.

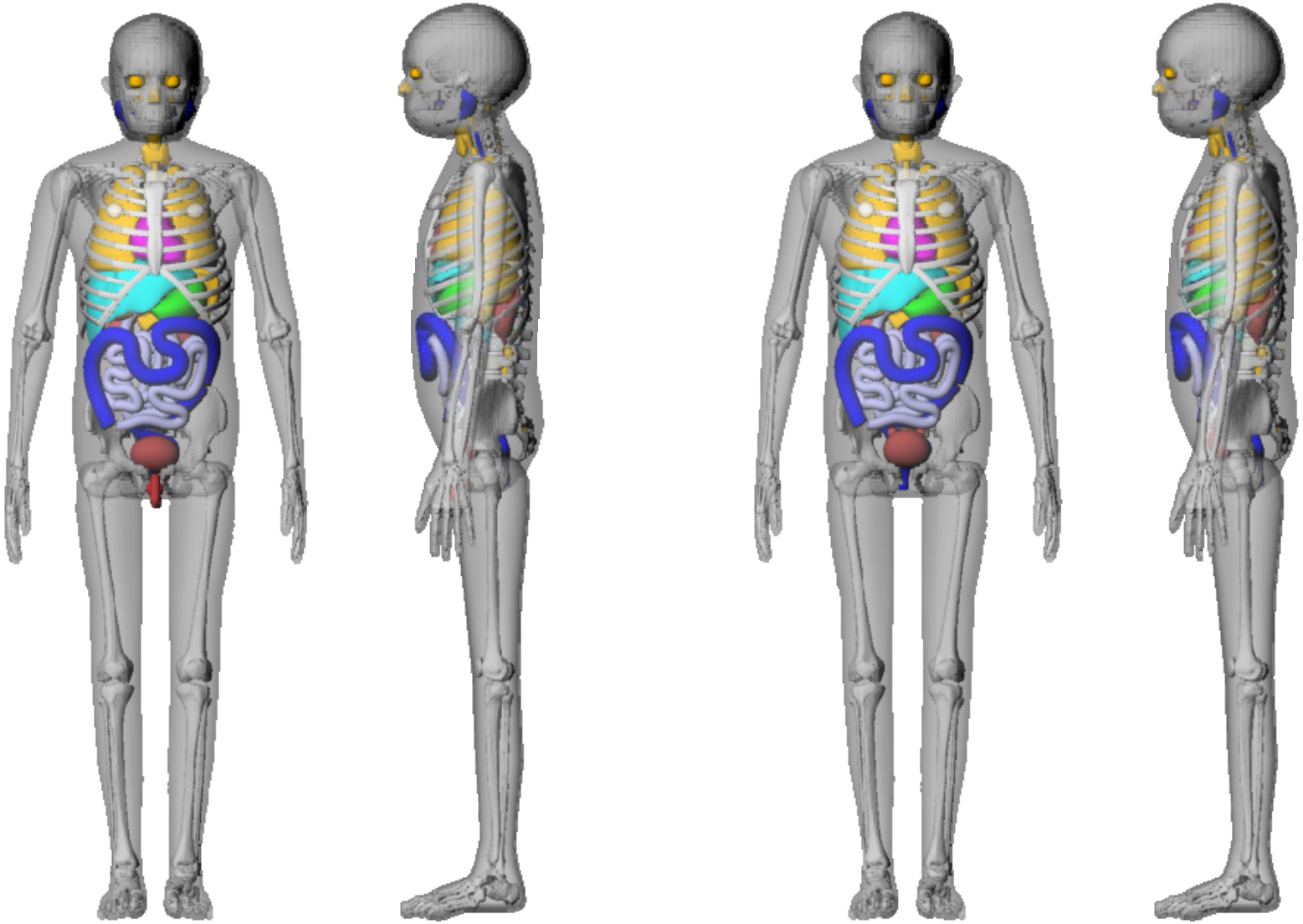

Figure 2-7. Anterior and lateral views of the 10 year male (left) and female (right) phantoms.

Table 2-1. Summary of CT examinations used for phantom development including CT imaging parameters and patient description.

Patient age (y)	Target age (y)	Gender	Examination type	Axial resolution (mm)	No. of axial images
1.7	1	F	C/A/P	3.00	116
2.3	1	F	Head	4.50	40
2.3	1	F	C-Spine	0.75	230
6.7	5	M	C/A/P	5.00	116
6.7	5	M	Head	4.50	36
11.2	10	F	C/A/P	6.00	97
12.3	10	F	Head	4.50	46
12.3	10	F	C-Spine	0.75	220

Table 2-2. Anthropometric reference values for the alimentary tract of 1, 5, and 10 year individuals and the resulting error in hybrid phantoms.

Reference data		***1 MF***	***5 MF***	***10 MF***
Length (cm)	Esophagus	13	18	23
	SI	120	170	220
	Right colon	18	23	28
	Left colon	21	26	31
	Rectosigmoid	21	26	31
UF hybrid phantoms				
Length (cm)	Esophagus	13.64	18.20	22.55
	SI	119.01	168.30	219.76
	Right Colon	19.51	23.44	27.04
	Left Colon	19.36	25.29	29.87
	Rectosigmoid	19.99	27.21	29.80
Percent error (%) - 5% tolerance				
	Esophagus	4.95	1.11	-1.96
	SI	-0.83	-1.00	-0.11
	Right colon	8.37	1.91	-3.44
	Left colon	-7.80	-2.73	-3.65
	Rectosigmoid	-4.82	4.65	-3.86

Table 2-3. Anthropometric reference values of 1, 5, and 10 year old individuals and resulting error in hybrid phantoms.

Anthropometric parameters		*Targeted values*			*UF hybrid phantoms*			*Percent difference*		
		1 MF	**5 MF**	**10 MF**	**1 MF**	**5 MF**	**10 MF**	**1 MF**	**5 MF**	**10 MF**
Height	Standing	76.0	109.0	138.0	75.8	109.6	139.4	-0.3	0.6	1.0
	Sitting	48.8	60.4	73.4	47.9	60.8	75.0	-1.9	0.7	2.3
Length	Total arm	32.6	47.1	61.0	32.0	47.6	62.0	-1.8	1.0	1.7
Circumference	Head	47.3	51.1	52.8	48.1	50.1	54.6	1.6	-2.0	3.4
	Neck		24.9	27.9		25.0	27.8		0.2	-0.3
	Waist		55.0	66.7		57.6	70.0		4.9	4.9
	Buttock		57.9	75.2		57.1	71.9		-1.3	-4.3
Breadth	Biacromial		25.0	31.2		24.1	29.7		-3.5	-4.5

Table 2-4. Organ masses for hybrid and voxel phantoms for 1 year male and female. Although separate male and female phantoms exist, values are listed collectively.

Organ System	Density	Comment	Target Volume	UFH - NURBS		UFH - Voxel		ICRP 89
	(g / cm^3)	(ICRU 46)	(cm^3)	mass (g)	% Diff	mass (g)	% Diff	mass (g)
Respiratory System								
ET1 (anterior nasal layer)	1.03	*ave soft tissue (male)*		0.14		0.14		ND
ET2 (posterior nasal layer)	1.03	*ave soft tissue (male)*		2.04		2.03		ND
ET2 (oral cavity layer)	1.03	*ave soft tissue (male)*		0.64		0.64		ND
ET2 (larynx)	1.07	*50:50 soft tissue/cartilage*	3.76	4.00	0.0%	3.97	-0.7%	4.00
ET2 (pharynx)	1.03	*ave soft tissue (male)*		0.84		0.82		ND
Trachea	1.07	*50:50 soft tissue/cartilage*	1.41	1.51	0.7%	1.50	0.0%	1.50
Bronchi - extrapulmonary	1.07	*50:50 soft tissue/cartilage*		2.17		2.15		ND
Lungs (inclusive of blood)	0.40	*calculated*		150.00	0.0%	149.91	-0.1%	150.00
Left Lung	0.40	*calculated*		69.36	-0.6%	69.32	-0.6%	69.77
Right Lung	0.40	*calculated*		80.64	0.5%	80.59	0.4%	80.23
Alimentary System								
Tongue	1.05	*muscle (newborn)*	9.52	10.06	0.6%	10.03	0.3%	10.00
Salivary glands	1.03	*ave soft tissue (male)*	23.30	23.98	-0.1%	23.93	-0.3%	24.00
Parotid	1.03	*ICRU-46 ave soft tissue*	13.59	14.0	-0.2%	13.9	-0.6%	14.00
Submaxillary	1.03	*ICRU-46 ave soft tissue*	6.80	7.0	0.0%	7.0	0.0%	7.00
Sublingual	1.03	*ICRU-46 ave soft tissue*	2.91	3.0	0.5%	3.0	0.4%	3.00
Tonsils	1.03	*ave soft tissue (male)*	0.49	0.50	0.0%	0.50	-0.1%	0.50
Esophagus - wall	1.03	*gastrointestine*	4.85	4.98	-0.4%	4.97	-0.5%	5.00
Stomach - wall	1.03	*gastrointestine*	19.42	20.04	0.2%	20.01	0.1%	20.00
Stomach - contents	1.03	*ave soft tissue (male)*	65.05	67.00	0%	66.79	-0.3%	67.00
Small Intestine - wall	1.03	*gastrointestine*	82.52	84.94	-0.1%	84.75	-0.3%	85.00
Small Intestine - contents	1.03	*ave soft tissue (male)*	90.29	37.96	-59%	37.86	-59.3%	93.00
Colon								
Right - wall	1.03	*gastrointestine*	19.42	20.09	0.5%	20.01	0.1%	20.00
Right - contents	1.03	*ave soft tissue (male)*	38.83	22.34	-44.1%	22.26	-44.3%	40.00
Left - wall	1.03	*gastrointestine*	19.42	19.95	-0.3%	19.91	-0.4%	20.00
Left - contents	1.03	*ave soft tissue (male)*	38.83	22.18	-44.6%	22.13	-44.7%	40.00
Rectosigmoid - wall	1.03	*gastrointestine*	9.71	10.01	0.1%	9.95	-0.5%	10.00
Rectosigmoid - contents	1.03	*ave soft tissue (male)*	19.42	22.97	14.8%	22.86	14.3%	20.00
Liver	1.05	*liver (40wk fetus)*	314.29	329.52	-0.1%	329.27	-0.2%	330.00
Gall Bladder - wall	1.03	*ave soft tissue (male)*	1.36	1.40	-0.3%	1.40	0.3%	1.40
Gall Bladder - contents	1.03	*ave soft tissue (male)*	7.77	8.01	0.1%	8.01	0.1%	8.00
Pancreas	1.03	*ave soft tissue (male)*	19.42	20.00	0.0%	19.91	-0.5%	20.00
Circulatory System								
Heart - wall	1.04	*heart (40wk fetus)*	48.08	50.18	0.4%	50.08	0.2%	50.00
Heart - content	1.06	*blood (newborn)*	45.28	47.99	0%	47.96	-0.1%	48.00
Urogenital System								
Kidneys (all regions)	1.04	*kidney (40wk fetus)*	67.31	69.89	-0.2%	69.81	-0.3%	70.00
Cortex (70%)	1.04	*kidney (fetus/child/adult)*	49.59	51.6	0.0%	51.5	-0.1%	51.58
Medulla (25%)	1.04	*kidney (fetus/child/adult)*	17.71	18.3	-0.5%	18.3	-0.6%	18.42
Pelvis (5%)	1.04	*bladder (adult-empty)*	3.54	3.7	-0.5%	3.7	-0.6%	3.68
Urinary Bladder - wall	1.04	*bladder (adult-empty)*	8.65	9.01	0.1%	8.97	-0.3%	9.00
Urinary Bladder - contents[a]	1.01	*urine of ave density*	31.68	10.11	-68.4%	11.00	-65.6%	32.00
Penis	1.05	*muscle (newborn)*		3.91		3.49		ND
Scrotum	1.03	*ave soft tissue (male)*		2.91		1.88		ND
Testes (2)	1.04	*testes (adult)*	1.44	1.50	0.0%	1.49	-0.9%	1.50
Prostate Gland	1.03	*ave soft tissue*	0.97	1.00	0.0%	1.00	-0.2%	1.00
Ovaries (2)	1.05	*ovaries (adult)*	0.76	0.80	0.0%	0.80	0.1%	0.80
Uterus	1.05	*ovaries (adult)*	1.43	1.50	0.1%	1.50	0.2%	1.50

[a] *No reference value is given in ICRP 89 and thus an approximate value is used as defined in the ORNL stylized newborn phantom*

Table 2-4. Continued

Organ System	Density (g / cm^3)	Comment (ICRU 46)	Target Volume (cm^3)	UFH - NURBS mass (g)	UFH - NURBS % Diff	UFH - Voxel mass (g)	UFH - Voxel % Diff	ICRP 89 mass (g)
Skeletal System								
Coastal Cartilage[b]	1.10	*volume-averaged*		26.2		23.5		
Intervertebral Discs[b]	1.10	*cortical bone (ICRP89 Para 436)*		10.8		10.8		
Bone Tissues	1.43	*effective ave density*	561.66	810.0	0.6%	812.00	0.9%	805.00
Bone (CB, TB)	1.66	*cortical bone (infant)*						590.00
Active Marrow[c]	1.03	*red marrow (adult)*						150.00
Inactive Marrow	0.98	*ICRU-46 ave soft tissue*						20.00
Miscellaneous[d]	1.03	*ave soft tissue (male)*						45.00
Integumentary System								
Skin[e]	1.10	*skin (newborn)*	318.18	ND		345.74	-1.2%	350.00
Additional Tissues								
Adrenal Glands (2)	1.03	*ave soft tissue (male)*	3.88	4.01	0.3%	4.01	0.1%	4.00
Brain	1.03	*brain (newborn)*	922.33	941.40	-0.9%	941.40	-0.9%	950.00
Breasts (2)	0.96	*adipose (newborn #2)*	ND	0.44		0.44		ND
Ears	1.10	*cartilage (adult)*		4.35		3.29		4.35
External nose	1.05	*66:33 soft tiss / cartilage*		2.83		2.02		2.83
Eyeballs (2)	1.03	*ave soft tissue (male)*	6.80	7.00	0.1%	6.97	-0.4%	7.00
Lens (2)	1.07	*eye lens (adult)*	0.20	0.21	0.3%	0.21	0.9%	0.21
Pituitary Gland	1.03	*ave soft tissue (male)*	0.15	0.15	0.0%	0.15	0.3%	0.15
Spinal Cord	1.04	*brain (newborn)*	ND	23.81		23.77		ND
Spleen	1.06	*spleen (40wk fetus)*	27.36	28.85	-0.5%	28.81	-0.7%	29.00
Thymus	1.03	*ICRP 89 - Para 606*	29.27	16.07	-46.4%	16.04	-46.5%	30.00
Thyroid	1.05	*thyroid (adult)*	1.71	1.80	0.0%	1.80	0.0%	1.80
Residual Soft Tissue	1.00	*effective ave density*	2509.17	ND		6646.29	0.3%	6623.5
Bone-Associated Cartilage	1.10							240.9
Separable Fat	0.96	*adipose (newborn #2)*						3600.00
Skeletal Muscle	1.05	*muscle (newborn)*						1900.00
Separable Connective Tissues	1.03	*ave soft tissue (male)*						350.00
Fixed Lymphatic Tissues[f]	1.03	*ave soft tissue (male)*						71.23
Blood (large vessels)[g]	1.06	*blood (newborn)*						137.38
Miscellaneous ROB[h]	1.03	*ave soft tissue (male)*						324.00
Totals by Organ System								
Respiratory System				161.34		161.17		155.5
Alimentary System - tissues of organ walls				569.45		568.57		569.9
Alimentary System - GI tract and gall bladder content				180.46		179.91		268.0
Circulatory System - heart wall and content				98.18		98.04		98.0
Urogenital System - kidneys and urinary bladder wall				78.90		78.78		79.0
Urogenital System - urinary bladder content				10.11		11.00		32.0
Urogenital System - internal sex organs (ovaries, uterus, prostate)[i]				3.30		3.30		3.30
Urogenital System - external sex organs (penis, scrotum, testes)				8.32		6.86		1.5
Skeletal System - bone tissues				810.00		812.00		805.0
Integumentary System				ND		345.74		350.0
Additional Tissues - excluding rest of body				1030.93		1028.92		1029.3
Additional Tissues - rest of body				ND		6646.29		6623.5
Total Body Tissues (F)						9743	0.3%	9714
Total Body Tissues (M)						9750	0.4%	9715
Total Body Mass (F)						9934	-0.8%	10014
Total Body Mass (M)						9941	-0.7%	10015

[b] *Skeletal cartilage excludes the following non-bone associated regions of cartilage: external nose and ears, larynx, trachea, and extrapulmonary bronchi*

[c] *Assumed to include the 7% of total blood volume in the newborn as per Section 7.7.2 of ICRP 89*

[d] *As per Section 9.2.15 of ICRP 89, miscellaneous skeletal tissues include periosteum and blood vessels, but exclude periarticular tissue and blood*

[e] *Skin masses given here are for the female phantom, and are 0.15% higher in the male phantom due to the addition of the penis and scrotum*

[f] *Estimated from the reference adult values given in Section 7.8.2 of ICRP Publication 89 and scaled by newborn to adult total body mass*

[g] *Taken as 25.92% of total blood pool as per Section 7.7.2 of ICRP 89 (other tissues, arota, large arteries, large veins)*

[h] *Miscellaneous rest-of-body is added to force the total body mass to its ICRP 89 reference value of 3500 g*

[i] *Male phantom masses additionally include soft tissuea occupied by the uterus and ovaries in the corresponding female phantom*

Table 2-5. Organ masses for hybrid and voxel phantoms for 5 year male and female. Although separate male and female phantoms exist, values are listed collectively.

Organ System	Density	Comment	Target Volume	UFH - NURBS		UFH - Voxel		ICRP 89
	(g / cm^3)	(ICRU 46)	(cm^3)	mass (g)	% Diff	mass (g)	% Diff	mass (g)
Respiratory System								
ET1 (anterior nasal layer)	1.03	*ave soft tissue (male)*		0.75		0.75		ND
ET2 (posterior nasal layer)	1.03	*ave soft tissue (male)*		17.25		17.25		ND
ET2 (oral cavity layer)	1.03	*ave soft tissue (male)*		1.32		1.32		ND
ET2 (larynx)	1.07	*50:50 soft tissue/cartilage*	6.57	6.60	0.4%	6.60	0.4%	7.00
ET2 (pharynx)	1.03	*ave soft tissue (male)*		1.06		1.06		ND
Trachea	1.07	*50:50 soft tissue/cartilage*	2.35	4.51	0.5%	4.51	92.2%	2.50
Bronchi - extrapulmonary	1.07	*50:50 soft tissue/cartilage*		3.62		3.62		ND
Lungs (inclusive of blood)	0.18	*calculated*	300.0	300.00	0.0%	300.00	0.0%	300.00
Left Lung	0.18	*calculated*		148.26		148.26		139.53
Right Lung	0.18	*calculated*		151.74		151.74		160.47
Alimentary System								
Tongue	1.05	*muscle (newborn)*	18.10	18.00	-0.6%	18.00	-0.6%	19.00
Salivary glands	1.03	*ave soft tissue (male)*	33.01	33.08	0.2%	33.08	0.2%	34.00
Parotid	1.03	*ICRU-46 ave soft tissue*	19.42	19.49	0.4%	19.49	0.4%	20.00
Submaxillary	1.03	*ICRU-46 ave soft tissue*	9.71	9.78	0.7%	9.78	0.7%	10.00
Sublingual	1.03	*ICRU-46 ave soft tissue*	3.88	3.88	0.0%	3.88	0.0%	4.00
Tonsils	1.03	*ave soft tissue (male)*	1.94	1.94	0.0%	1.94	0.0%	2.00
Esophagus - wall	1.03	*gastrointestine*	9.71	9.61	-1.0%	9.61	-1.0%	10.00
Stomach - wall	1.03	*gastrointestine*	48.54	48.44	-0.2%	48.44	-0.2%	50.00
Stomach - contents	1.03	*ave soft tissue (male)*	80.58	81.27	0.9%	81.27	0.9%	83.00
Small Intestine - wall	1.03	*gastrointestine*	213.59	214.28	0.3%	214.28	0.3%	220.00
Small Intestine - contents	0.59	*ave soft tissue (male)*	199.45	200.14	0.3%	200.14	0.3%	117.00
Colon								
Right - wall	1.03	*gastrointestine*	47.57	47.60	0.1%	47.60	0.1%	49.00
Right - contents	0.82	*ave soft tissue (male)*	60.94	61.05	0.2%	61.05	0.2%	50.00
Left - wall	1.03	*gastrointestine*	47.57	48.00	0.9%	48.00	0.9%	49.00
Left - contents	0.33	*ave soft tissue (male)*	76.00	76.10	0.1%	76.10	0.1%	25.00
Rectosigmoid - wall	1.03	*gastrointestine*	21.36	21.22	-0.7%	21.22	-0.7%	22.00
Rectosigmoid - contents	0.37	*ave soft tissue (male)*	67.22	67.22	0.0%	67.22	0.0%	25.00
Liver	1.05	*liver (40wk fetus)*	542.86	544.05	0.2%	544.05	0.2%	570.00
Gall Bladder - wall	1.03	*ave soft tissue (male)*	2.52	2.52	-0.2%	2.52	-0.2%	2.60
Gall Bladder - contents	1.03	*ave soft tissue (male)*	14.56	14.48	-0.6%	14.48	-0.6%	15.00
Pancreas	1.03	*ave soft tissue (male)*	33.98	34.12	0.4%	34.12	0.4%	35.00
Circulatory System								
Heart - wall	1.04	*heart (40wk fetus)*	81.73	82.42	0.8%	82.42	0.8%	85.00
Heart - content	1.06	*blood (newborn)*	127.36	128.05	0.5%	128.05	0.5%	135.00
Urogenital System								
Kidneys (all regions)	1.04	*kidney (40wk fetus)*	105.77	106.46	0.7%	106.46	0.7%	110.00
Cortex (70%)	1.04	*kidney (fetus/child/adult)*	77.93	78.62	0.9%	78.62	0.9%	81.05
Medulla (25%)	1.04	*kidney (fetus/child/adult)*	27.83	27.68	-0.5%	27.68	-0.5%	28.95
Pelvis (5%)	1.04	*bladder (adult-empty)*	5.57	5.58	0.2%	5.58	0.2%	5.79
Urinary Bladder - wall	1.04	*bladder (adult-empty)*	15.38	15.38	0.0%	15.38	0.0%	16.00
Urinary Bladder - contents[a]	1.01	*urine of ave density*	61.39	62.08	1.1%	62.08	1.1%	62.00
Penis	1.05	*muscle (newborn)*		1.58		1.58		ND
Scrotum	1.03	*ave soft tissue (male)*		0.69		0.69		ND
Testes (2)	1.04	*testes (adult)*	1.63	1.63	0.0%	1.63	0.0%	1.70
Prostate Gland	1.03	*ave soft tissue*	1.17	1.17	0.0%	1.17	0.0%	1.20
Ovaries (2)	1.05	*ovaries (adult)*	1.90	1.89	-0.7%	1.89	-0.7%	2.00
Uterus	1.05	*ovaries (adult)*	2.86	2.87	0.5%	2.87	0.5%	3.00

[a] *No reference value is given in ICRP 89 and thus an approximate value is used as defined in the ORNL stylized newborn phantom*

Table 2-5. Continued

Organ System	Density (g/cm^3)	Comment (ICRU 46)	Target Volume (cm^3)	UFH - NURBS mass (g)	UFH - NURBS % Diff	UFH - Voxel mass (g)	UFH - Voxel % Diff	ICRP 89 mass (g)
Skeletal System								
Coastal Cartilage[b]	1.10	*volume-averaged*		57.5		57.5		
Intervertebral Discs[b]	1.10	*cortical bone (ICRP89 Para 436)*		73.1		73.1		
Bone Tissues	1.41	*effective ave density*	1297.03	1304.6	0.6%	1304.6	0.6%	1830.00
Bone (CB, TB)	1.70	*cortical bone (infant)*						1260.00
Active Marrow[c]	1.03	*red marrow (adult)*						340.00
Inactive Marrow	0.98	*ICRU-46 ave soft tissue*						160.00
Teeth	1.65							15.00
Miscellaneous[d]	1.03	*ave soft tissue (male)*						55.00
Integumentary System								
Skin[e]	1.10	*skin (newborn)*	518.18	ND		520.0	0.4%	570.00
Additional Tissues								
Adrenal Glands (2)	1.03	*ave soft tissue (male)*	4.85	4.86	0.2%	4.9	0.2%	5.00
Brain	1.04	*brain (newborn)*	1197.12	1197.00	0.0%	1197.0	0.0%	1245.00
Breasts (2)	0.96	*adipose (newborn #2)*	ND	4.20		4.2		ND
Ears	1.10	*cartilage (adult)*		1.32		1.3		5.58
External nose	1.05	*66:33 soft tiss / cartilage*		2.38		2.4		7.32
Eyeballs (2)	1.03	*ave soft tissue (male)*	10.68	10.64	-0.4%	10.6	-0.4%	11.00
Lens (2)	1.07	*eye lens (adult)*	0.31	0.31	0.0%	0.3	0.0%	0.33
Pituitary Gland	1.03	*ave soft tissue (male)*	0.24	0.24	0.0%	0.2	0.0%	0.25
Spinal Cord	1.04	*brain (newborn)*	ND	18.68		18.7		ND
Spleen	1.06	*spleen (40wk fetus)*	47.17	47.18	0.0%	47.2	0.0%	50.00
Thymus	1.03	*ICRP 89 - Para 606*	29.27	29.15	-0.4%	29.1	-0.4%	30.00
Thyroid	1.05	*thyroid (adult)*	3.24	3.25	0.3%	3.2	0.3%	3.40
Residual Soft Tissue	1.01	*effective ave density*	2509.17	ND		2500.0	-0.4%	11878.80
Bone-Associated Cartilage	1.10							528.3
Separable Fat	0.96	*adipose (newborn #2)*						5000.00
Skeletal Muscle	1.05	*muscle (newborn)*						5600.00
Separable Connective Tissues	1.03	*ave soft tissue (male)*						700.00
Fixed Lymphatic Tissues[f]	1.03	*ave soft tissue (male)*						190.00
Blood (large vessels)[g]	1.06	*blood (newborn)*						388.80
Miscellaneous ROB[h]	1.03	*ave soft tissue (male)*						0.00
Totals by Organ System								
Respiratory System				340.52		340.52		309.5
Alimentary System - tissues of organ walls				1700.54		1700.54		1096.6
Alimentary System - GI tract and gall bladder content				360.00		360.00		315.0
Circulatory System - heart wall and content				369.84		369.84		220.0
Urogenital System - kidneys and urinary bladder wall				204.76		204.76		126.0
Urogenital System - urinary bladder content				98.94		98.94		62.0
Urogenital System - internal sex organs (ovaries, uterus, prostate)[i]				1.60		1.60		6.20
Urogenital System - external sex organs (penis, scrotum, testes)				12.20		12.20		1.7
Skeletal System - bone tissues				3773.74		3773.74		1830.0
Integumentary System				ND		ND		570.0
Additional Tissues - excluding rest of body				1548.19		1548.19		1357.9
Additional Tissues - rest of body				ND		ND		11878.8
Total Body Tissues (F)						16726		17395
Total Body Tissues (M)						16728		17397
Total Body Mass (F)						17088		17772
Total Body Mass (M)						17090		17774

[b] *Skeletal cartilage excludes the following non-bone associated regions of cartilage: external nose and ears, larynx, trachea, and extrapulmonary bronchi*

[c] *Assumed to include the 7% of total blood volume in the newborn as per Section 7.7.2 of ICRP 89*

[d] *As per Section 9.2.15 of ICRP 89, miscellaneous skeletal tissues include periosteum and blood vessels, but exclude periarticular tissue and blood*

[e] *Skin masses given here are for the female phantom, and are 0.15% higher in the male phantom due to the addition of the penis and scrotum*

[f] *Estimated from the reference adult values given in Section 7.8.2 of ICRP Publication 89 and scaled by newborn to adult total body mass*

[g] *Taken as 25.92% of total blood pool as per Section 7.7.2 of ICRP 89 (other tissues, arota, large arteries, large veins)*

[h] *Miscellaneous rest-of-body is added to force the total body mass to its ICRP 89 reference value of 3500 g*

[i] *Male phantom masses additionally include soft tissue occupied by the uterus and ovaries in the corresponding female phantom*

Table 2-6. Organ masses for hybrid and voxel phantoms for 10 year male and female. Although separate male and female phantoms exist, values are listed collectively.

Organ System	Density	Comment	Target Volume	UFH - NURBS		UFH - Voxel		ICRP 89
	(g / cm^3)	(ICRU 46)	(cm^3)	mass (g)	% Diff	mass (g)	% Diff	mass (g)
Respiratory System								
ET1 (anterior nasal layer)	1.03	*ave soft tissue (male)*		0.75		0.67		ND
ET2 (posterior nasal layer)	1.03	*ave soft tissue (male)*		17.25		17.28		ND
ET2 (oral cavity layer)	1.03	*ave soft tissue (male)*		1.32		1.39		ND
ET2 (larynx)	1.07	*50:50 soft tissue/cartilage*	11.27	12.03	0.2%	12.01	0.1%	12.00
ET2 (pharynx)	1.03	*ave soft tissue (male)*		1.06		1.05		ND
Trachea	1.07	*50:50 soft tissue/cartilage*	4.23	4.52	0.4%	4.48	-0.3%	4.50
Bronchi - extrapulmonary	1.07	*50:50 soft tissue/cartilage*		3.62		3.54		ND
Lungs (inclusive of blood)	0.32	*calculated*		500.00	0.0%	498.40	-0.3%	500.00
Left Lung	0.32	*calculated*		250.76	7.8%	249.87	7.4%	232.56
Right Lung	0.32	*calculated*		249.24	-6.8%	248.53	-7.1%	267.44
Alimentary System								
Tongue	1.05	*muscle (newborn)*	30.48	32.02	0.1%	31.83	-0.5%	32.00
Salivary glands	1.03	*ave soft tissue (male)*	42.72	43.99	0.0%	43.88	-0.3%	44.00
Parotid	1.03	*ICRU-46 ave soft tissue*	25.24	26.0	0.0%	25.9	-0.3%	26.00
Submaxillary	1.03	*ICRU-46 ave soft tissue*	12.62	13.0	0.0%	13.0	-0.3%	13.00
Sublingual	1.03	*ICRU-46 ave soft tissue*	4.85	5.0	0.0%	5.0	-0.4%	5.00
Tonsils	1.03	*ave soft tissue (male)*	2.91	3.00	0.0%	2.99	-0.4%	3.00
Esophagus - wall	1.03	*gastrointestine*	17.48	18.00	0.0%	17.94	-0.3%	18.00
Stomach - wall	1.03	*gastrointestine*	82.52	84.85	-0.2%	84.68	-0.4%	85.00
Stomach - contents	1.03	*ave soft tissue (male)*	113.59	116.99	0%	116.02	-0.8%	117.00
Small Intestine - wall	1.03	*gastrointestine*	359.22	370.53	0.1%	368.69	-0.4%	370.00
Small Intestine - contents	0.82	*ave soft tissue (male)*	199.45	163.00	0%	162.54	-0.3%	163.00
Colon								
Right - wall	1.03	*gastrointestine*	82.52	85.09	0.1%	84.85	-0.2%	85.00
Right - contents	1.15	*ave soft tissue (male)*	60.94	70.00	0.0%	69.90	-0.1%	70.00
Left - wall	1.03	*gastrointestine*	82.52	85.05	0.1%	84.70	-0.3%	85.00
Left - contents	0.46	*ave soft tissue (male)*	76.00	35.00	0.0%	34.86	-0.4%	35.00
Rectosigmoid - wall	1.03	*gastrointestine*	38.83	40.00	0.0%	39.75	-0.6%	40.00
Rectosigmoid - contents	0.52	*ave soft tissue (male)*	67.22	35.00	0.0%	34.83	-0.5%	35.00
Liver	1.05	*liver (40wk fetus)*	790.48	829.63	0.0%	828.71	-0.2%	830.00
Gall Bladder - wall	1.03	*ave soft tissue (male)*	4.27	4.40	-0.1%	4.41	0.2%	4.40
Gall Bladder - contents	1.03	*ave soft tissue (male)*	25.24	26.01	0.0%	25.97	-0.1%	26.00
Pancreas	1.03	*ave soft tissue (male)*	58.25	59.99	0.0%	59.89	-0.2%	60.00
Circulatory System								
Heart - wall	1.04	*heart (40wk fetus)*	134.62	140.45	0.3%	140.05	0.0%	140.00
Heart - content	1.06	*blood (newborn)*	216.98	229.38	0%	229.20	-0.3%	230.00
Urogenital System								
Kidneys (all regions)	1.04	*kidney (40wk fetus)*	173.08	179.72	-0.2%	179.44	-0.3%	180.00
Cortex (70%)	1.04	*kidney (fetus/child/adult)*	127.53	132.4	-0.2%	132.2	-0.3%	132.63
Medulla (25%)	1.04	*kidney (fetus/child/adult)*	45.55	47.3	-0.1%	47.3	-0.2%	47.37
Pelvis (5%)	1.04	*bladder (adult-empty)*	9.11	9.5	0.1%	9.5	-0.1%	9.47
Urinary Bladder - wall	1.04	*bladder (adult-empty)*	24.04	25.03	0.1%	24.91	-0.4%	25.00
Urinary Bladder - contents[a]	1.01	*urine of ave density*	98.02	98.94	-0.1%	98.61	-0.4%	99.00
Penis	1.05	*muscle (newborn)*		8.23		8.18		ND
Scrotum	1.03	*ave soft tissue (male)*		1.98		2.82		ND
Testes (2)	1.04	*testes (adult)*	1.92	2.00	-0.1%	1.99	-0.5%	2.00
Prostate Gland	1.03	*ave soft tissue*	1.55	1.60	0.0%	1.59	-0.4%	1.60
Ovaries (2)	1.05	*ovaries (adult)*	3.33	3.49	-0.1%	3.47	-0.8%	3.50
Uterus	1.05	*ovaries (adult)*	3.81	4.00	0.1%	3.99	-0.3%	4.00

[a] *No reference value is given in ICRP 89 and thus an approximate value is used as defined in the ORNL stylized newborn phantom*

Table 2-6. Continued

Organ System	Density	Comment	Target Volume	UFH - NURBS		UFH - Voxel		ICRP 89
	(g / cm^3)	(ICRU 46)	(cm^3)	mass (g)	% Diff	mass (g)	% Diff	mass (g)
Skeletal System								
Coastal Cartilage[b]	1.10	*volume-averaged*		57.5		55.2		
Intervertebral Discs[b]	1.10	*cortical bone (ICRP89 Para 436)*		73.1		67.9		
Bone Tissues	1.38	*effective ave density*	2674.35	3680.4	0.0%	3665.76	-0.4%	3680.00
Bone (CB, TB)	1.75	*cortical bone (infant)*						2300.00
Active Marrow[c]	1.03	*red marrow (adult)*						630.00
Inactive Marrow	0.98	*ICRU-46 ave soft tissue*						630.00
Teeth	1.65							30.00
Miscellaneous[d]	1.03	*ave soft tissue (male)*						90.00
Integumentary System								
Skin[e]	1.10	*skin (newborn)*	745.45	ND		0.00	-100.0%	820.00
Additional Tissues								
Adrenal Glands (2)	1.03	*ave soft tissue (male)*	6.80	7.01	0.2%	7.00	0.0%	7.00
Brain	1.04	*brain (newborn)*	1259.62	1309.99	0%	1309.61	0.0%	1310.00
Breasts (2)	0.96	*adipose (newborn #2)*	ND	7.65		7.63		ND
Ears	1.10	*cartilage (adult)*		5.58		5.54		5.58
External nose	1.05	*66:33 soft tiss / cartilage*		7.32		6.89		7.32
Eyeballs (2)	1.03	*ave soft tissue (male)*	11.65	11.99	-0.1%	11.92	-0.7%	12.00
Lens (2)	1.07	*eye lens (adult)*	0.34	0.36	0.5%	0.36	0.1%	0.36
Pituitary Gland	1.03	*ave soft tissue (male)*	0.34	0.35	0.2%	0.35	0.1%	0.35
Spinal Cord	1.04	*brain (newborn)*	ND	72.49		69.95		ND
Spleen	1.06	*spleen (40wk fetus)*	75.47	80.01	0.0%	79.81	-0.2%	80.00
Thymus	1.03	*ICRP 89 - Para 606*	36.59	37.53	0.1%	37.49	0.0%	37.50
Thyroid	1.05	*thyroid (adult)*	7.52	7.90	0.0%	7.89	-0.2%	7.90
Residual Soft Tissue	1.02	*effective ave density*	2509.17	ND		23736.03	4.6%	22684.33
Bone-Associated Cartilage	1.10							427.3
Separable Fat	0.96	*adipose (newborn #2)*						7500.00
Skeletal Muscle	1.05	*muscle (newborn)*						11000.00
Separable Connective Tissues	1.03	*ave soft tissue (male)*						1100.00
Fixed Lymphatic Tissues[f]	1.03	*ave soft tissue (male)*						320.00
Blood (large vessels)[g]	1.06	*blood (newborn)*						648.00
Miscellaneous ROB[h]	1.03	*ave soft tissue (male)*						1689.00
Totals by Organ System								
Respiratory System				540.56		538.82		516.5
Alimentary System - tissues of organ walls				1700.54		1696.20		1700.4
Alimentary System - GI tract and gall bladder content				446.00		444.13		446.0
Circulatory System - heart wall and content				369.84		369.25		370.0
Urogenital System - kidneys and urinary bladder wall				204.76		204.34		205.0
Urogenital System - urinary bladder content				98.94		98.61		99.0
Urogenital System - internal sex organs (ovaries, uterus, prostate)[i]				9.10		9.05		9.10
Urogenital System - external sex organs (penis, scrotum, testes)				12.20		12.99		2.0
Skeletal System - bone tissues				3680.43		3665.76		3680.0
Integumentary System				ND		0.00		820.0
Additional Tissues - excluding rest of body				1548.19		1544.44		1468.0
Additional Tissues - rest of body				ND		23736.03		22684.3
Total Body Tissues (F)						31764	1.0%	31453
Total Body Tissues (M)						31777	1.0%	31455
Total Body Mass (F)						32307	1.0%	31998
Total Body Mass (M)						32320	1.0%	32000

[b] *Skeletal cartilage excludes the following non-bone associated regions of cartilage: external nose and ears, larynx, trachea, and extrapulmonary bronchi*

[c] *Assumed to include the 7% of total blood volume in the newborn as per Section 7.7.2 of ICRP 89*

[d] *As per Section 9.2.15 of ICRP 89, miscellaneous skeletal tissues include periosteum and blood vessels, but exclude periarticular tissue and blood*

[e] *Skin masses given here are for the female phantom, and are 0.15% higher in the male phantom due to the addition of the penis and scrotum*

[f] *Estimated from the reference adult values given in Section 7.8.2 of ICRP Publication 89 and scaled by newborn to adult total body mass*

[g] *Taken as 25.92% of total blood pool as per Section 7.7.2 of ICRP 89 (other tissues, arota, large arteries, large veins)*

[h] *Miscellaneous rest-of-body is added to force the total body mass to its ICRP 89 reference value of 3500 g*

[i] *Male phantom masses additionally include soft tissuea occupied by the uterus and ovaries in the corresponding female phantom*

CHAPTER 3
CONCLUSIONS

Both stylized (equation-based) and tomographic (image-based) phantoms have traditionally been used for assessment of radiation dose. Each of these has a particular forte. Stylized phantoms remain more flexible and easier to use, while voxel phantoms are more realistic of human beings. The UFH phantoms developed combine both of these features into one.

The direct segmentation of CT or MRI images results in a phantom that realistically depicts complex organ shapes. Furthermore, the use of NURBS surfaces in the UFH phantoms allows for a wide range of organ scalability. This technology allowed for creation of the 1, 5, and 10 year phantoms that are at the reference values for 8 different anthropometric measures, several different alimentary tract lengths, and at the ICRP masses for nearly all organs. In particular, the resourcefulness of this modeling technique was highlighted in the modeling of the alimentary tract. Previous segmentation methods required exact recognition of the soft tissue boundaries of the wall of the intestine in order to correctly model the GI tract. However, by using the central track of the lumen and fitting NURBS surfaces around it, the intestines and colon were able to be modeled in each of the phantoms using a pipe surface and the reference mass for each of these organs was matched within ± 1%. It is important to note that the GI contents were not matched to within 1% of ICRP reference values. However, these values are susceptible to the food intake and digestive rates of each individual, which makes the masses highly variable.

Moreover, this method of surface modeling lends the phantom to further uses. The freely deformable surfaces allow for scaling of the phantom to non reference dimensions. This would allow the user to utilize these phantoms in modeling of cases such as non-50^{th} percentile individuals by height (overly tall or short) or weight (underweight or overweight) for radiation

protection or medical dose assessment studies. The ease of NURBS surfaces could also allow for the modeling of disease states of an organ or modeling a solid tumor in the body. Further studies should be implemented to analyze these issues to expand the knowledge of radiation protection to a larger portion of the total population.

LIST OF REFERENCES

Cristy M, and Eckerman KF 1987 Specific absorbed fractions of energy at various ages from internal photon sources. Oak Ridge, TN: Oak Ridge National Laboratory. ORNL/TM-8381/Volumes I-VII

ICRP 2002 Basic anatomical and physiological data for use in radiological protection: reference values. New York, New York: International Commission on Radiological Protection. Publication 89

ICRP 2006 Human alimentary tract model for radiological protection. Oxford; Pergamon Press: International Commission on Radiological Protection. ICRP Publication 100

ICRU 1992 Photon, electron, proton and neutron interaction data for body tissues. Bethesda, MD: International Commission on Radiation Units and Measurements. Report 46

Kramer R, Khoury HJ, Vieira JW, Loureiro EC, Lima VJ, Lima FR, and Hoff G 2004a All about FAX: a Female Adult voXel phantom for Monte Carlo calculation in radiation protection dosimetry. Phys Med Biol **49**(23) 5203-16

Kramer R, Vieira JW, Khoury HJ, and Lima FD 2004b MAX meets ADAM: a dosimetric comparison between a voxel-based and a mathematical model for external exposure to photons. Physics in Medicine and Biology **49**(6) 887-910

Kramer R, Zankl M, Williams G, and Drexler G 1982 The calculation of dose from external photon exposures using reference human phantoms and Monte-Carlo methods, Part 1: The male (ADAM) and female (EVA) adult mathematical phantoms. Neuherberg, Germany: GSF-National Research Center for Health and Environment. GSF Bericht S-885

Kuczmarski RJ, Ogden CL, Guo SS, Grummer-Strawn LM, Flegal KM, Mei Z, Wei R, Curtin LR, Roche AF, and Johnson CL 2002 2000 Growth Charts for the Unites States: improvements to the 1977 National Center for Health Statistics version. Pediatrics **109** 45-60

Lee C, Lee C, Williams JL, and Bolch WE 2006 Whole-body voxel phantoms of paediatric patients - UF Series B. Phys Med Biol **51**(17) 4649-4661

Lee C, Lodwick D, Hasenauer D, Williams JL, Lee C, and Bolch WE 2007 Hybrid computational phantoms of the male and female newborn patient: NURBS-based whole-body models. Phys Med Biol **52**(12) 3309-3333

Nipper JC, Williams JL, and Bolch WE 2002 Creation of two tomographic voxel models of pediatric patients in the first year of life. Phys Med Biol **47**(11) 3143-3164

Pazik FD, Staton RJ, Hintenlang DE, Arreola MM, Williams JL, and Bolch WE 2007 Organ and effective doses in newborns and infants undergoing voiding cystourethrograms (VCUG): A comparison of stylized and tomographic phantoms. Med Phys **34**(1) 294-306

Segars WP, Lalush DS, and Tsui BMW 2001 Modeling respiratory mechanics in the MCAT and spline-based MCAT phantoms. Ieee Transactions on Nuclear Science **48**(1) 89-97

Segars WP, and Tsui BM 2002 Study of the efficacy of respiratory gating in myocardial SPECT using the new 4D NCAT phantom. IEEE Trans Nucl Sci **49**(3) 675-679

Slyper AH 1998 Childhood obesity, adipose tissue distribution, and the pediatric practitioner. Pediatrics **102** e4 (electronic version)

Snyder WS, Ford MR, Warner GG, and Fisher HL 1969 Estimates of absorbed fractions for monoenergetic photon sources uniformly distributed in various organs of a heterogeneous phantom. New York: Society of Nuclear Medicine. MIRD Pamphlet No. 5

Stabin M, Watson E, Cristy M, Ryman J, Eckerman K, Davis J, Marshall D, and Gehlen M 1995 Mathematical models and specific absorbed fractions of photon energy in the nonpregnant adult female and at the end of each trimester of pregnancy. Oak Ridge, TN: Oak Ridge National Laboratory. ORNL/TM-12907

Zhang S-x 1999 An atlas of histology. New York: Springer

BIOGRAPHICAL SKETCH

Daniel Lee Lodwick was born in Columbus, Ohio, in 1984. Daniel is the son of David and Kathy Lodwick. Daniel graduated from Royal Palm Beach Community High School in 2002 and attended the University of Florida thereafter. In fall 2006, he earned his B.S. in nuclear engineering and graduated summa cum laude. Daniel is currently enrolled in the College of Engineering and pursuing his Master of Science degree in nuclear engineering sciences.